Khulna University Studies **Volume 21(1): 268-280: 2024**

REVIEW ARTICLE **SCIENCE & ENGINEERING**

SEVERE CYCLONIC STORM SITRANG: A METEOROLOGICAL ANALYSIS OF ITS FORMATION, INTENSITY, AND IMPACT ON BANGLADESH

Mohammad Wahiduzzaman[1]* and Gour Chandra Paul[2]

[1]*Mathematics Discipline, Khulna University, Khulna 9208, Bangladesh*
[2]*Department of Mathematics, University of Rajshahi, Rajshahi 6205, Bangladesh*

KUS: 973: 25042023

Manuscript submitted: April 25, 2023 Accepted: May 2, 2024

Abstract

Employing a non-central difference method of lines in tandem with the 4th order Runge-Kutta technique, this study adopts a sophisticated computational approach, ensuring precision and efficiency to resolve the shallow water equations and predict water levels caused by a cyclone in the coastal area of Bangladesh. To discretize spatial derivatives, a 4-point backward finite difference method utilized while keeping time derivatives continuous. The authors transformed the shallow water equations with boundary conditions into an initial value problem and used the Runge-Kutta(4,4) method for solving this transformed initial value problem. To effectively include the land-sea boundary and bottom structure at a reasonable charge, the authors used a high-resolution approach. To create a regular and stable tidal oscillation in the area, the authors applied the M_2 tidal component to the southern boundary of the primary model. Then ran the surge model to estimate water elevations caused by the nonlinear interaction between tide and surge. Using numerical experiments, the authors simulated water heights generated by tide, pure surge, and tide surge interaction caused by the intense cyclonic storm SITRANG. The study's simulated results demonstrate a commendable alignment with the reported data.

Keywords: SITRANG, Bay of Bengal, Cyclonic storm, High resolution approach.

Introduction

As stated in a source [1], storm surge refers to a phenomenon that occurs when the sea level increases or decreases as a result of alterations in wind stress and atmospheric pressure. As per [2], there are approximately five occurrences of storm surges with a height of 5 meters or more in the Bay of Bengal (BoB) every ten years. Over the past century, the BoB has witnessed the formation of 508 cyclones, among them, 17% of the cyclones hit Bangladesh's landmass., resulting approximately 80% of losses in both human lives and property across the globe were recorded [3,4]. The CoB is distinguished by unique features, such as an extensive continental shelf with shallow depths, a coastline with a shape resembling a funnel, abundant islands located off the coast, a complex boundary between land and sea, along with low-lying areas inland [5-7]. While the IIT Kharagpur model can precisely forecast water levels resulting from meteorological conditions [8], the BMD meteorologists rely on global models to predict total water levels. However, since global models cannot account due to the complications that occur in a specific region, the accuracy of water level predictions is significantly affected [9]. Furthermore, the BMD meteorologists rarely make further modifications to the models [10, 11]. The authors of the cited study [10] rely on speculative predictions of water levels based on wind speed and ancient statistical models. Therefore, researchers are actively pursuing more reliable numerical models to provide accurate information for the CoB. Several numerical modeling studies have been conducted for storm surges in this region, including [3, 10, 12-18] while many of these studies have used explicit or semi-implicit FDM, it is crucial to comply with the CFL stability conditions to maintain stability, this approach can be both computationally expensive and accuracy limiting. As a result, researchers are seeking economic and accurate alternatives, such as the method of lines (MOLs), which offer stability advantages and lower computational costs [7]. The use of MOLs in storm surge modeling along the CoB was first introduced by [14] with the use of a 3-point central FDM for discretization of spatial derivatives with the RK(4,4) process for solving ODEs. However, subsequent studies by [5-

*Corresponding author: <wahid@math.ku.ac.bd>
DOI: https://doi.org/10.53808/KUS.2024.21.01.973-se

7, 24-25] made use of a more sophisticated time integrator, while still utilizing the same 3PCFDM for spatial derivative discretization. It is worth noting that higher-order FDMs for spatial derivative discretization can lead to improved results [19], and higher-order backward FDMs are particularly effective when used with MOLs [20]. Taking this into account, the present study employs a four-point backward finite difference method (4PBFDM) to discretize spatial derivatives, without affecting time derivatives, by applying non-central backward FDM. The system of ordinary differential equations (ODEs) that results is solved using the RK(4,4) technique. Implementation of 4PBFDM along with RK(4,4) provides an enhancement over the methodology used in [14].

Model equations

In order to investigate the dynamic processes taking place in the sea [18], utilizing the equations;

$$\frac{\partial \xi}{\partial t} = \frac{-\partial}{\partial x}[(\xi + h)u] - \frac{\partial}{\partial y}[(\xi + h)v], \tag{1}$$

$$\frac{\partial u}{\partial t} = -u\frac{\partial u}{\partial x} - v\frac{\partial u}{\partial y} + fv - g\frac{\partial \xi}{\partial x} + \frac{\tau_x}{\rho(\xi+h)} - C_f\frac{u(u^2+v^2)^{1/2}}{\xi+h}, \tag{2}$$

$$\frac{\partial v}{\partial t} = -u\frac{\partial v}{\partial x} - v\frac{\partial v}{\partial y} - fu - g\frac{\partial \xi}{\partial y} + \frac{\tau_y}{\rho(\xi+h)} - C_f\frac{v(u^2+v^2)^{1/2}}{\xi+h}. \tag{3}$$

In this particular research, the computational xy-plane is established with the origin positioned at 23° N, 85° E as shown in Figure 1. The x-axis is defined as a south-directed line, while the y-axis represents an eastward stripe. The x and y components of velocity, denoted by u and v, respectively. The variable $\xi(x, y, t)$ represents the water level deviations, either above or below the average sea level (MSL), at the free surface., and the undisturbed depth of the water is indicated by the function $h(x, y)$. The Coriolis parameter, $f = 2\,\Omega\,sin\phi$, is determined by the angular speed of the earth rotation, Ω, and the latitude of the location of interest, ϕ, expressed in degrees. The acceleration caused by gravity at a particular location, denoted by, g (= 9.81 m/s^2), and the seawater density, ρ, which is assumed to be uniform, are also considered in the research. In addition, a dimensionless bottom friction coefficient, C_f, is used, and the wind stress acting on the sea surface is represented by the x and y components denoted as T_x and T_y respectively.

Similar to the methodology utilized in [14], the boundary conditions are expressed as follows:
For the western boundary located at 85° E, the open boundary is defined by

$$v + \sqrt{\frac{g}{h}}\xi = 0. \tag{4}$$

Similarly, for the eastern boundary positioned at 95° E, the open boundary is

$$v - \sqrt{\frac{g}{h}}\xi = 0. \tag{5}$$

For the southern boundary located at 15° N, the open boundary is described by

$$u - \sqrt{\frac{g}{h}}\xi = -2a\sqrt{\frac{g}{h}}sin\left(\frac{2\pi t}{T} + \phi\right). \tag{6}$$

where the amplitude, period, and phase of the tidal constituent are represented by a, T, and φ, respectively.

Furthermore, in accordance with the methodology proposed in [21], Incorporated into our analysis is the estimation of the Meghna River's fresh water discharge, utilizing the child scheme approach, along the open section of the northern boundary at 23° N latitude. Let Q be the volumetric flow rate of freshwater river discharge over time, and let B be its corresponding width in meters, then;

$$u_b = u + \frac{Q}{B(h+\xi)}. \tag{7}$$

The wind stress is the main driver of the storm surge model, and it can be expressed as x and y components, as shown in [7]:

$$(T_x, T_y) = \rho_a C_D|V_a|(u_a, v_a); |V_a| = (u_a^2 + v_a^2)^{1/2}, \tag{8}$$

The surface wind's x and y components can be expressed as u_a and v_a, correspondingly. According to [7], we assume C_D in the following form:

$$C_D = \begin{cases} 1.052 \times 10^{-3} \text{ when } |V_a| \le 6 \text{ ms}^{-1} \\ 0.638 \times 10^{-3} + 0.609 \times 10^{-3} \text{ when } 6 < |V_a| < 30 \text{ ms}^{-1} \\ 2.708 \times 10^{-3} \text{ when } |V_a| \ge 30 \text{ ms}^{-1} \end{cases} \quad (9)$$

Utilizing the formula provided in reference [22], we can produce the wind field as

$$V_a = \begin{cases} V_0\sqrt{(r_a/R)^3} \text{ for all } r_a \le R \\ V_0\sqrt{(R/r_a)^3} \text{ for all } r_a \ge R\text{'} \end{cases} \quad (10)$$

Within the given context, V_0 denotes the maximum wind speed (MSWS) at the farthest radial distance, R, from the center of the cyclone, whereas r_a refers to the distance between the cyclone's center and the specified location within the wind field.

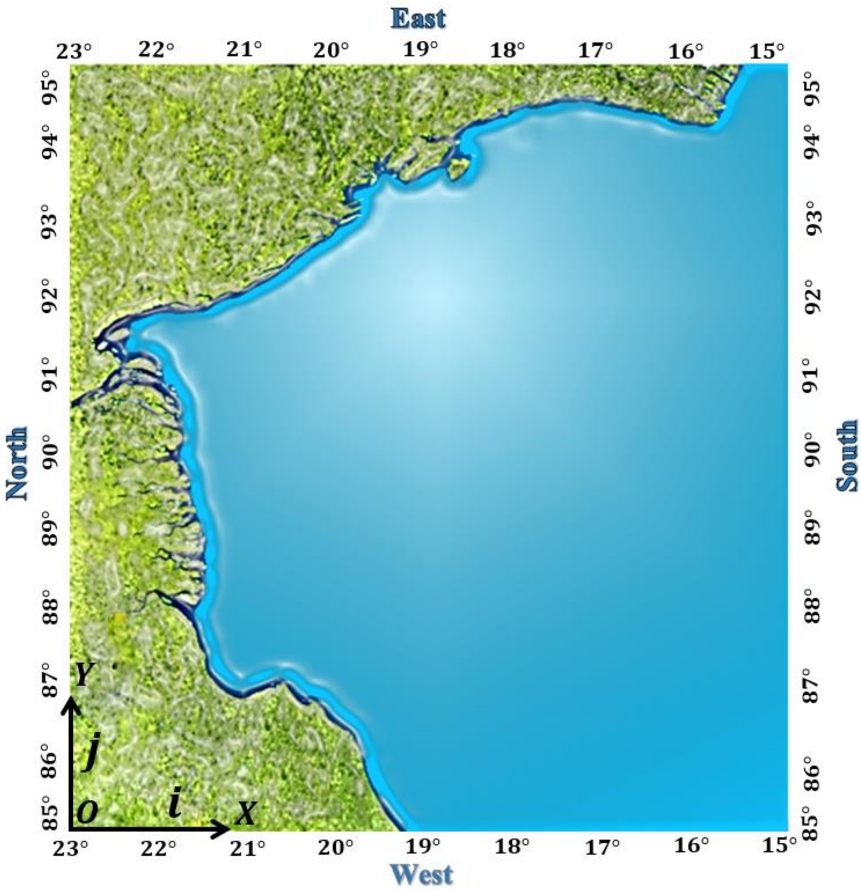

Figure 1. Boundaries of the physical domain along with the coordinate system.

Discretization of the governing equations

To discretize the governing equations, we can use the notation $A_{i,j}^k$ to represent the dependent variable $A(x_i, y_j, t_k)$ at a grid point (x_i, y_j) and time t_k. Then, we can use the following notations:

$\overline{A_{i,j}^k}^x = 0.5\left(A(x_{i+1}, y_j, t^k) + A(x_{i-1}, y_j, t^k)\right)$, $\overline{A_{i,j}^k}^y = 0.5\left(A(x_i, y_{j+1}, t^k) + A(x_i, y_{j-1}, t^k)\right)$,

$\overline{A_{i,j}^k}^{xy} = 0.25\left(A(x_{i+1}, y_{j+1}, t^k) + A(x_{i+1}, y_{j-1}, t^k) + A(x_{i-1}, y_{j+1}, t^k) + A(x_{i-1}, y_{j-1}, t^k)\right)$,

Using these notations, equations (1)-(6) can be written as:

$$\left(\frac{\partial \xi}{\partial t}\right)_{i,j} = CR1 + CR2, \quad (11)$$

DOI: https://doi.org/10.53808/KUS.2024.21.01.973-se

where, $CR1 = -\frac{1}{6\,\Delta x}[z_1 - 6z_2 + 3z_3 + 2z_4]$ and $CR2 = -\frac{1}{6\,\Delta y}[z_5 - 6z_6 + 3z_7 + 2z_8]$,

Here,

$$z_1 = \begin{cases} \left(\xi_{i-2,j} + h_{i-2,j}\right)\overline{u_{i-2,j}}^x, & \text{when } i \neq 2 \\ \left(3\,\xi_{i,j} - 2\,\xi_{i+2,j} + 1.25\,h_{i,j} - 0.25\,h_{i+1,j}\right)\left(1.25\,u_{i-1,j} - 0.25\,u_{i+1,j}\right) & \text{otherwise} \end{cases}$$

$$z_2 = \begin{cases} \left(\overline{\xi_{i-1,j}}^x + h_{i-1,j}\right)u_{i-1,j}, & \text{when } i \neq 2 \\ \left(1.25\,\xi_{i,j} - 0.25\,\xi_{i+2,j} + h_{i-1,j}\right)u_{i-1,j} & \text{otherwise} \end{cases}$$

$$z_3 = \left(\xi_{i,j} + h_{i,j}\right)\overline{u_{i,j}}^x,\ z_4 = \left(\overline{\xi_{i+1,j}}^x + h_{i+1,j}\right)u_{i+1,j}$$

$$z_5 = \begin{cases} \left(\xi_{i,j-2} + h_{i,j-2}\right)\overline{u_{i,j-2}}^y, & \text{when } j \neq 3 \\ \left(\xi_{i,j-2} + h_{i,j-2}\right)\left(1.25\,u_{i,j-1} - 0.25\,u_{i,j+1}\right) & \text{otherwise} \end{cases}$$

$$z_6 = \left(\overline{\xi_{i,j-1}}^y + h_{i,j-1}\right)u_{i,j-1},\ z_7 = \left(\xi_{i,j} + h_{i,j}\right)\overline{u_{i,j}}^y,\ z_8 = \left(\overline{\xi_{i,j+1}}^y + h_{i,j+1}\right)u_{i,j+1}.$$

From Eq. (2),

$$\left(\frac{\partial u}{\partial t}\right)_{i,j} = UR1 + UR2 + UR3 + UR4 + UR5 + UR6, \tag{12}$$

In Eq. (12),

$$UR1 = -u_{ij}\,[x_1 - 6x_2 + 3x_3 + 2x_4]/6\Delta x,$$

$$UR2 = -\overline{v_{ij}}^{xy}\,[x_5 - 6x_6 + 3x_7 + 2x_8]/6\Delta y,\ UR3 = f_i\,\overline{v_{ij}}^{xy},$$

$$UR4 = -g\,[x_9 - 6x_{10} + 3x_{11} + 2x_{12}]/6\Delta x,$$

$$UR5 = -\frac{C_f\,u_{i,j}^k}{\overline{\xi_{i,j}^{k+1}}^x + h_{i,j}}\left(\left(u_{i,j}^k\right)^2 + \left(\overline{v_{i,j}^k}^{xy}\right)^2\right) \text{ and } UR6 = \frac{\tau_x}{\rho\left(\overline{\xi_{i,j}^{k+1}}^x + h_{i,j}\right)},$$

where

$$x_1 = u_{i-2,j},\ x_2 = 0.5\,(u_{i-2,j} + u_{i,j}),\ x_3 = u_{i,j},$$

$$x_4 = \begin{cases} 0.5\,\left(u_{i+2,j} + u_{i,j}\right) & \text{when } i \neq m-1 \\ 1.25\,u_{i,j} - 0.25\,u_{i-2,j} & \text{otherwise} \end{cases}$$

$$x_5 = u_{i,j-2},\ x_6 = 0.5(u_{i,j-2} + u_{i,j}),\ x_7 = u_{i,j},\ x_8 = 0.5(u_{i,j+2} + u_{i,j}),$$

$$x_9 = \begin{cases} 0.5\left(\xi_{i-3,j} + \xi_{i-1,j}\right) & \text{when } i \neq 3 \\ 1.25\,\xi_{i-1,j} - 0.25\,\xi_{i+1,j} & \text{otherwise} \end{cases},$$

$$x_{10} = \xi_{i-1,j},\ x_{11} = 0.5(\xi_{i-1,j} + \xi_{i+1,j}),\ x_{12} = \xi_{i+1,j}.$$

To maintain conciseness, we exclude the discretization procedure for the v-component of the momentum equation, as it is similar to that of the u-component.

The raises at $j = 1, j = N$, and $i = M$ can be figured from the boundary conditions (Eqs. (4)-(6)). Specifically, the elevation at $j = 1$ is computed in one way, the elevation at $j = N$ is computed in another way, and the elevation at $i = M$ is computed in a third way.

$$\xi_{i,1}^{k+1} = \xi_{i,3}^{k+1} - 2\sqrt{\frac{h_{i,2}}{g}}\,v_{i,2}^k, \tag{13}$$

$$\xi_{i,N}^{k+1} = \xi_{i,N-2}^{k+1} + 2\sqrt{\frac{h_{i,N-1}}{g}}\,v_{i,N-1}^k, \tag{14}$$

$$\xi_{M,j}^{k+1} = \xi_{M-2,j}^{k+1} + 2\sqrt{\frac{h_{M-1,j}}{g}}\,v_{M-1,j}^k + 4a\,sin\left(\frac{2\pi t}{T} + \phi\right), \tag{15}$$

where $i = 2, 4, 6, \ldots, M-2$ and $j = 1, 3, 5, \ldots, N$.

Now, Eq. (7) result as

$$(u_b)_{1,j}^{k+1} = u_{3,j}^{k+1} + \frac{Q}{(\overline{\xi_{3,j}^{k+1}}^x + h_{3,j})B}, \quad \text{where } j = 53, 54, 55. \tag{16}$$

To numerically integrate the ODE scheme specified by Eqs. (13)-(15), an RK(4,4) time integrator is employed, taking into account various parameters and input data provided. The first step involves the solution of Eq. (13) through RK(4,4) method to update the water height ξ at diverse grid nodes, while adhering to the Arakawa C-grid approach [23]. Subsequently, the updated ξ values are applied to the (even, odd) nodes in the CMS borders, using the boundary conditions (Eqs. (14)-(16)). To determine the values of ξ at every other water grid node, a technique of inverse distance weighted averaging is utilized. Eventually, the ξ values are computed at the land-sea interface grid points. To generate the storm track, data is collected from BMD, and wind stress is calculated using Eq. (9) with relevant parameter values obtained from Eq. (10).

Life cycle of SITRANG

During late October 2022, a tropical cyclone by the name of SITRANG (as shown in Fig. 2) had an impact on India and Bangladesh. Despite being classified as a weak cyclone, it still had significant effects. On October 22nd, SITRANG had its genesis in the waters off the Andaman and Nicobar Islands and gradually gained strength, ultimately reaching its peak in the capacity of a severe tropical cyclone. On October 25th, during the early hours, SITRANG made landfall near Barisal in Bangladesh.

The meteorological history of SITRANG

A low-pressure area was detected in the North Andaman Sea, as well as adjacent regions of the South Andaman Sea and Southeast BoB on October 20th, 2022, according to meteorologists. By October 21st, the low-pressure area had gradually intensified into a well-marked low-pressure (WMLP) region over the North Andaman Sea and connecting Southeast BoB due to favorable environmental conditions. On October 22nd, a depression (D) formed over Southeast and attached East Central BoB near the Andaman Islands due to these conditions. The depression then shifted northwestwards and strengthened into a deep depression (DD) over West Central BoB on October 23rd, before transforming into Cyclonic Storm SITRANG later that day. By the evening of October 23rd, SITRANG had become a cyclonic storm and started to gradually recurve north-northeastwards. It made landfall on Bangladesh's coast between Tinkona and Sandwip, near Barisal, during the night of October 24th, with MSWS of 80-90 km/h up to 100 km/h. On October 24th, it declining into a DD over northeast Bangladesh and further into a depression over interior Bangladesh on October 25th. Finally, it turned into a WMLP over northeast Bangladesh and attached Meghalaya on October 25th. The cyclone SITRANG path can be observed in Figure 3.

Salient Features

Cyclonic Storm SITRANG's development and landfall had unique characteristics. Firstly, it followed a recurving path that moved north-west initially due to the impact of south-eastern winds at central and higher tropospheric stages. Subsequently, the system gradually changed its course towards north-northeast due to the impact of a trough in westerlies and an anticyclone towards its east over Myanmar. Secondly, the storm exhibited a rapid pace on the 24th, influenced by a westerly trough, an anticyclone over Myanmar, and connections with land. Its average speed was around 21.8 kmph, which was faster than the average 12.9 km/h for cyclonic storms over the BoB during the post-monsoon season. During landfall, the storm moved at a speed of about 50 km/h. Finally, Cyclonic Storm SITRANG had a relatively short life span compared to the long period average (LPA) for the Bay of Bengal's post-monsoon season cyclonic storm category, lasting about 69 hours compared to the LPA of about 3 days and 16 hours.

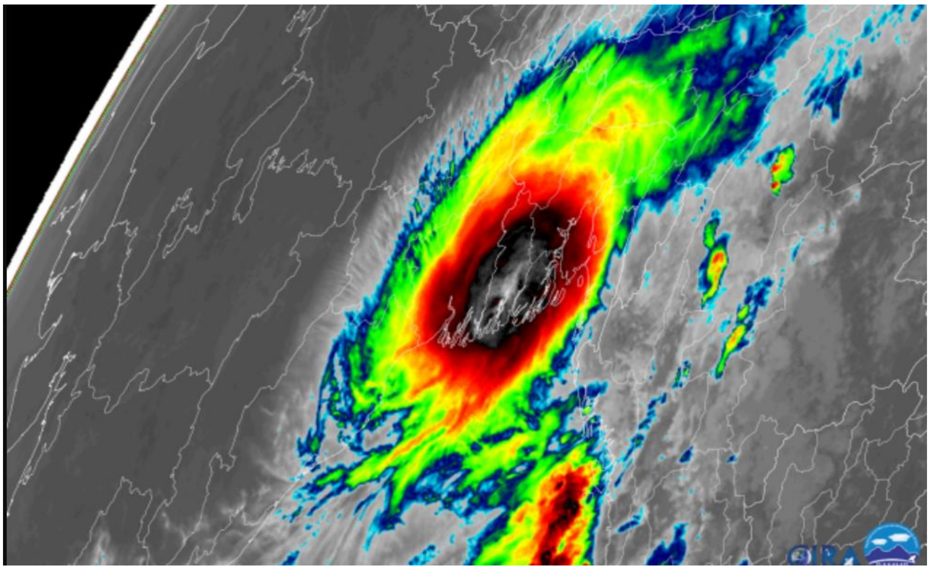

Figure 2. Infrared satellite imagery shows Cyclonic Storm SITRANG as it makes landfall in Bangladesh on Monday, Oct. 24, 2022. CIRA/RAAMB

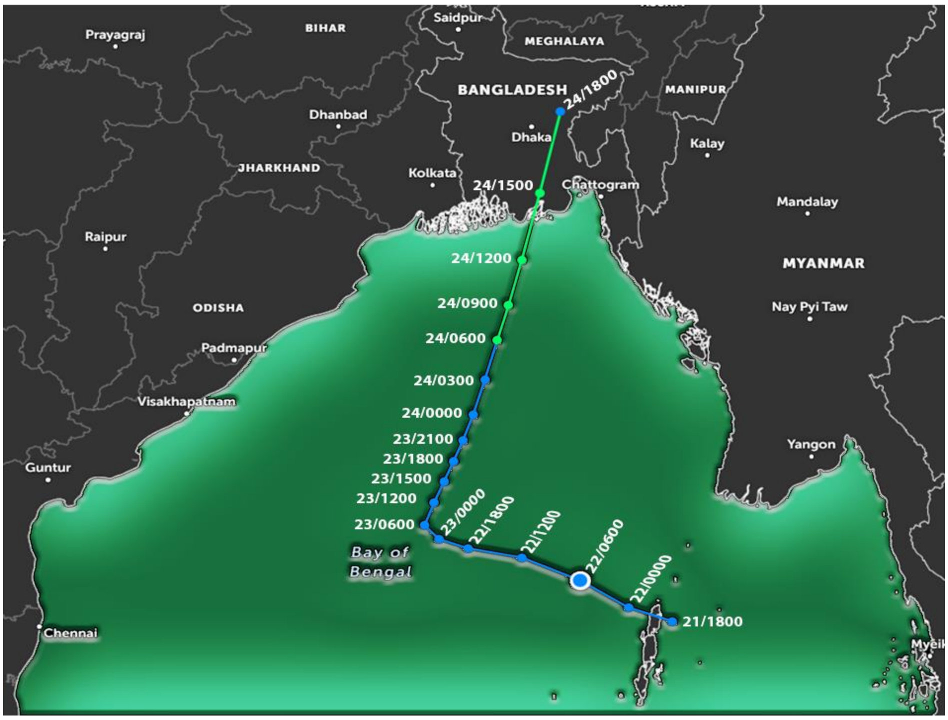

Figure 3. Path followed by Cyclonic Storm 'SITRANG' over the Bay of Bengal from October 22nd to 24th, 2022.

Table 1. Time-varying information (21-24 October, 2022) of TC SITRANG (IMD).

Date	Time	Position		Type	Wind	Pressure
UTC		Lat. ºN	Long. ºE		m/s	hPa
Oct 21	18:00	13.20	93.30	D	15	-
Oct 22	00:00	13.50	92.40	D	15	-
Oct 22	06:00	14.10	91.40	D	15	-
Oct 22	12:00	14.60	90.20	D	15	-
Oct 22	18:00	14.80	89.10	D	15	-
Oct 23	00:00	15.00	88.50	D	15	-
Oct 23	06:00	15.30	88.20	D	15	-
Oct 23	12:00	15.80	88.40	DD	20	998
Oct 23	15:00	16.26	88.60	DD	20	998
Oct 23	18:00	16.70	88.80	DD	20	998
Oct 23	21:00	17.15	88.99	DD	20	997
Oct 24	00:00	17.70	89.20	DD	20	997
Oct 24	03:00	18.45	89.44	DD	20	998
Oct 24	06:00	19.30	89.70	C	20	999
Oct 24	09:00	20.04	89.93	C	20	999
Oct 24	12:00	21.00	90.20	C	25	999
Oct 24	15:00	22.41	90.57	C	20	996
Oct 24	18:00	24.10	91.00	DD	20	994

Source: https://zoom.earth/storms/sitrang-2022/#map=daily

On October 22nd, 2022, a cyclonic storm was formed and it dissipated on October 25th, 2022. The highest sustained winds recorded for 3 minutes were 85 km/h (50 mph), while for 1 minute, it was 110 km/h (50 mph). The storm had a maximum sustained wind radius of 25000 meters, and the lowest pressure recorded was 994 hPa (mbar) or 29.35 inHg.

The study area with numerical estimation

The area of interest for this study is situated between latitudes 15°-23° N and longitudes 85°-95° E (Fig. 1) and spans approximately 9,35,568 sq km. The large size of this area allows for a tropical cyclone (TC) to remain present for at least three days before making landfall, providing ample time to issue warnings and mitigate damage caused by storm surges. In order to compute the scalar component ξ, even-odd nodes are used on the numerical xy-plane, while u and v are kept at odd-odd and even-even nods, respectively. The coastal and island boundaries in the area are estimated using a technique called the stair-step representation, as depicted in Figure 4. This approach involves approximating the shoreline and island perimeters as a series of straight lines that resemble a staircase. By doing so, the curvature of the coast and islands can be approximated reasonably well, even though the actual shoreline and island boundaries may be more complex. This method allows for a simplified representation of the coastal and island boundaries, making it easier to incorporate them into the simulation models, whereby it is approximated by connecting the nearest odd y-directed lines and even x-directed lines. The study employs the course mesh scheme (CMS) across the entire area of interest, with a fine mesh scheme (FMS) injected to accommodate complex coastal boundaries and bottom topography. The FMS is designed to provide accurate approximations of the complex land-sea interface. To account for the densely populated, low-lying islands between Barisal and Chittagong, and the highly curved coastline, a very fine mesh scheme (VFMS) is nested within the FMS. Figure 5(a-c) and Table 2 provides information on numerical calculations.

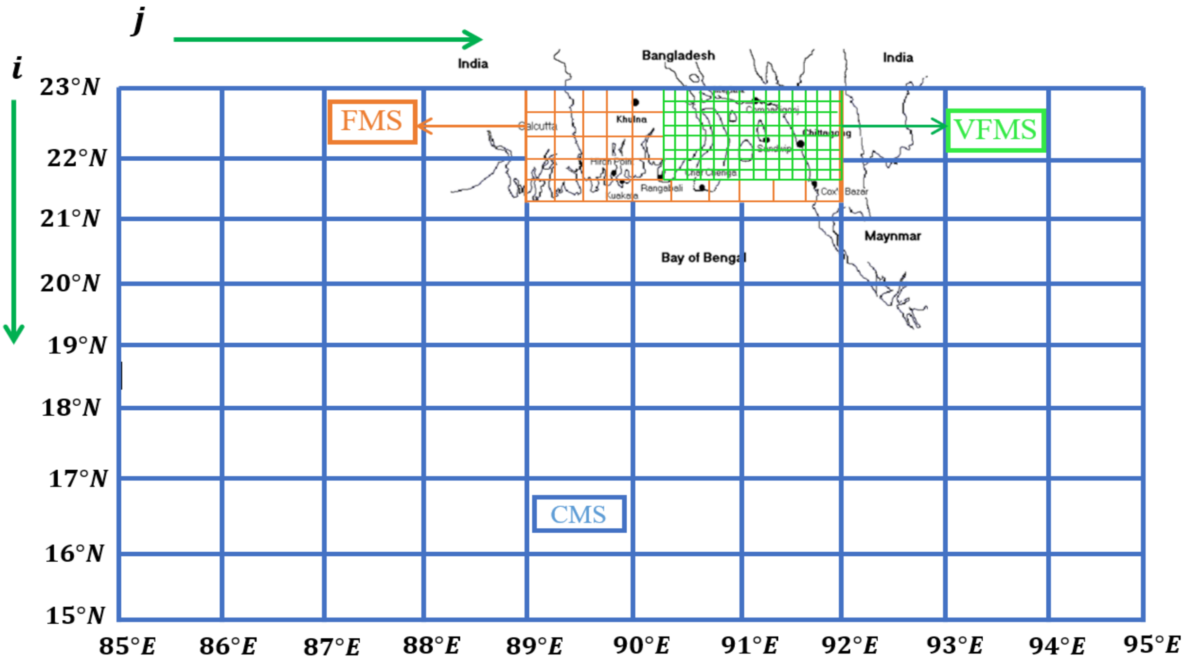

Figure 4. Visualization of the nested scheme in the physical domain.

Table 2. The step-size and domains of different schemes with computational grids.

Scheme	Domain extent	Step size along x-axis	Step size along y-axis	Number of grid points
CMS	15^0 to 23^0 N and 85^0 to 93^0 E	15.08 km	17.52 km	60×61
FMS	21.15^0 to 23^0 N and 89^0 to 92^0 E	2.15 km	3.29 km	92×95
VFGM	21.77^0 N to 23^0 N and 90.40^0 E to 92^0 E	720.73 m	1142.39 m	190 × 145

(a) CMS: Domain: 15^o-23^o N and 85^o-93^o E, Number of grid points: 60×61, Step size: x=15.08 km, y=17.52 km.

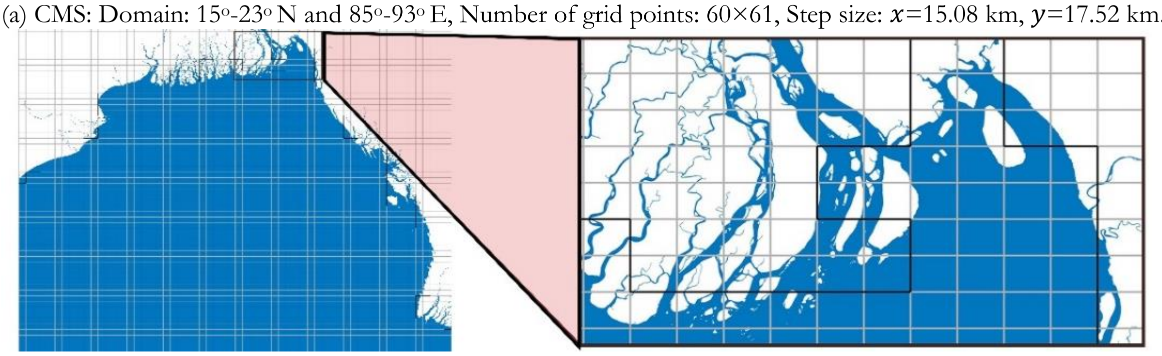

(b) FMS: Domain: 21.15°-23° N and 85°-93° E, Number of grid points: 92×95, Step size: x=2.15 km, y=3.29 km.

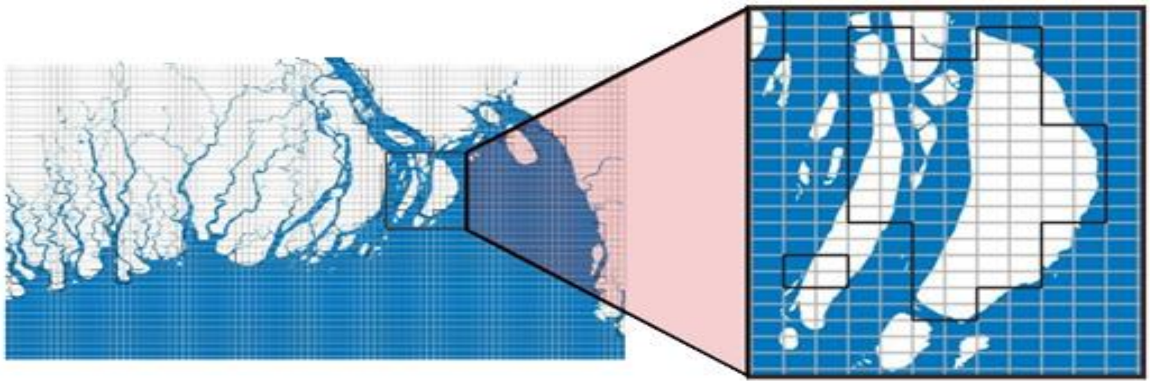

(c) VFMS: Domain: 21.77°-23° N and 90.40°-92° E, Number of grid points: 190×145, Step size: x=720.73 m, y=1142.39 m.

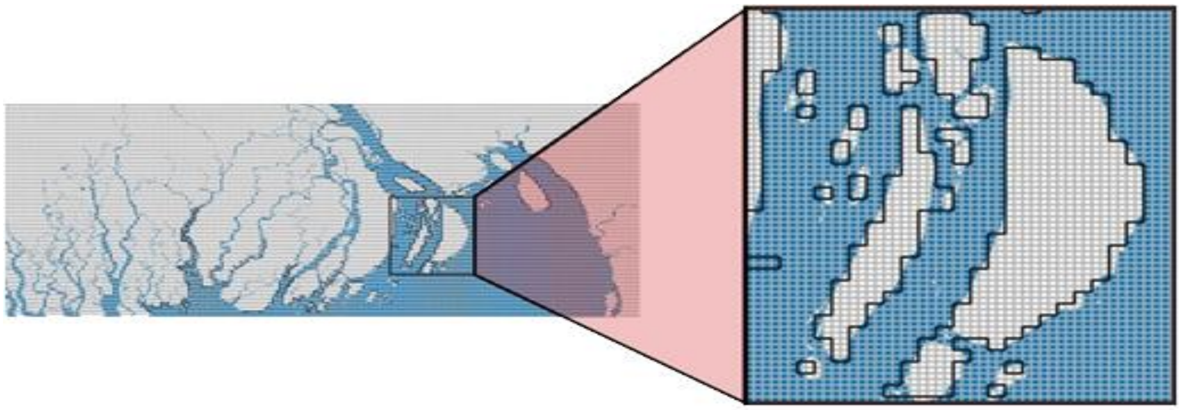

Figure 5 (a-c). Stair-step representation in the physical domain with grid spacing and number of computational points of different schemes.

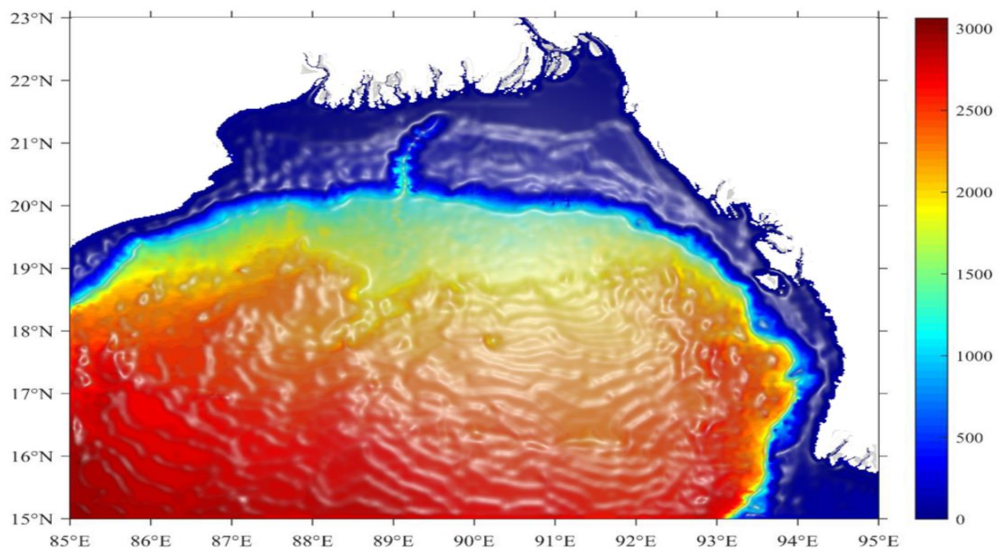

Figure 6. Our generated bathymetric figure through Shepard interpolation from which water depth is compiled.

Discussion of results

The study involved running simulations for 80 hours, and the results were recorded over the final 48 hours at multiple locations, including both coastal and islands areas. To present our findings, we selected seven stations that are representative of the Ganges tidal plain and the Chittagong straight plane The tidal outcomes in relation to the mean sea level (MSL) at these locations are illustrated in Figures 7-10.

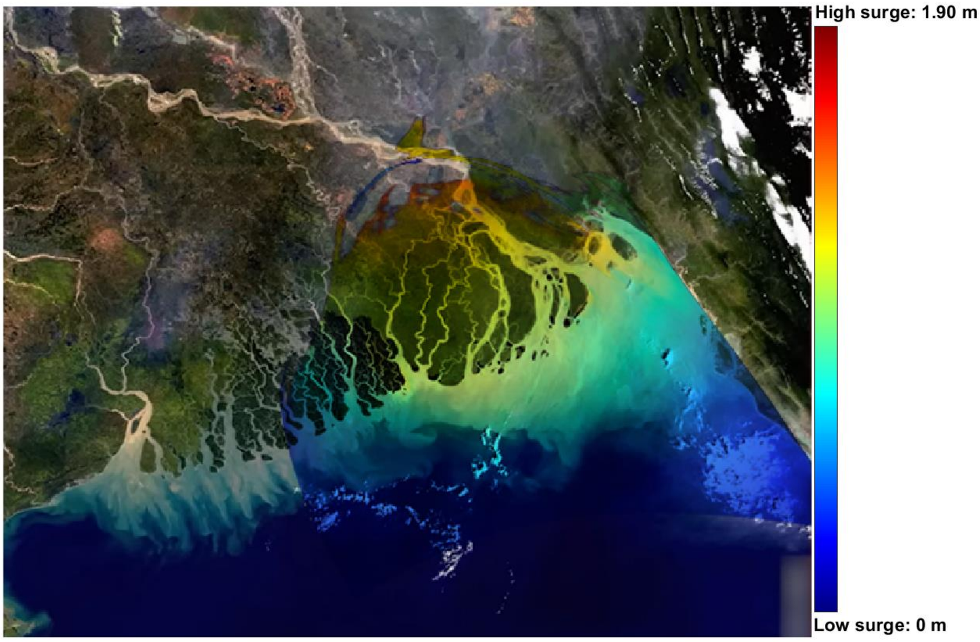

Figure 7. Projected tidal wave due to CS SITRANG.

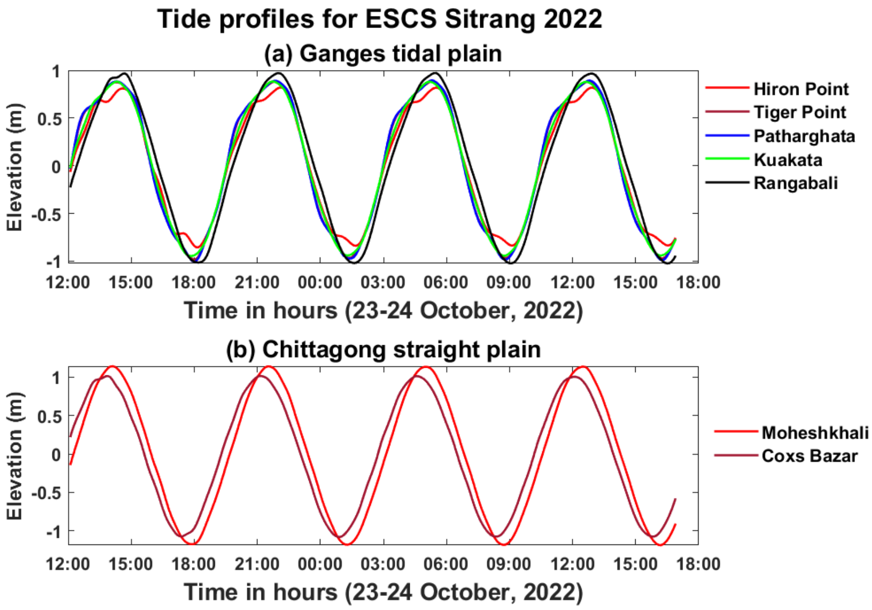

Figure 8(a-b). Tide profiles for ESCS SITRANG at Ganges tidal plain and Chittagong straight plain.

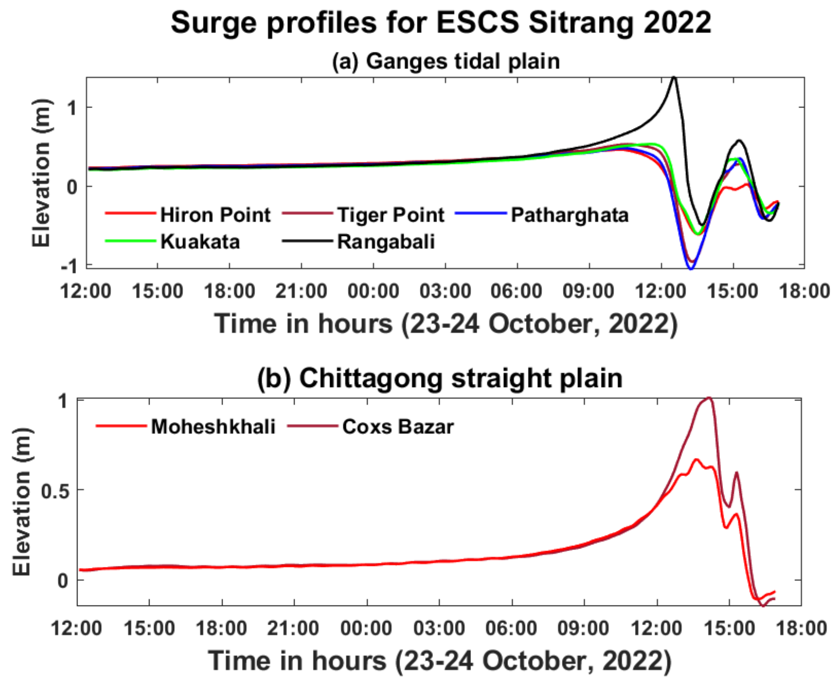

Figure 9(a-b). Surge profiles for ESCS SITRANG at Ganges tidal plain and Chittagong straight plain.

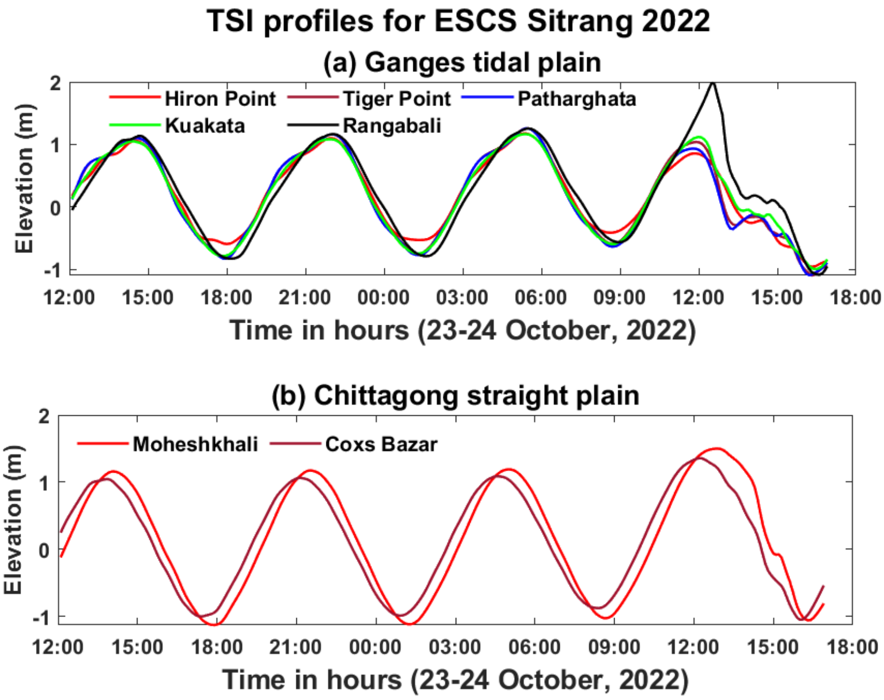

Figure 10(a-b). TSI profiles for ESCS SITRANG at Ganges tidal plain and Chittagong straight plain.

This warning was issued when the system was at the deep depression stage, which was roughly 60 hours before landfall. Another warning was issued on 23rd October (0630 UTC) for the West Bengal coast concerning a storm surge of about 1 meter overhead astronomical tide. The Sitakund area of Bangladesh experienced the extreme storm surge of approximately 1.7 m above astronomical tide, while the highest surge of around 0.5 m (Fig. 7). The funneling form of the head Bay of Bengal led to the peak surge near Sitakund, which occurred roughly 130 km away from the cyclone's landfall point in a rightward direction.

Conclusion

In this research article, a new model is presented that combines the non-central MOL approach with the RK(4,4) technique to predict WLs generated by TCs along the coastal regions of Bangladesh. The model's computed WLs are found to be in good agreement with the data collected from the BIWTA and other similar studies. The research demonstrates that the track and intensity of a TC significantly impact the total WLs. While the model does have some limitations, they are considered reasonable for such complex numerical computations. The authors aim to address some of these limitations in future studies. It is also noteworthy that non-central MOLs of order six or higher can replicate the results.

Conflict of interest

The authors state that they have no competing interests related to the publication of this paper.

References

Ahmmed. S. F., 2010. MHD Visco-Elestic Boundary Layer Flow of Fluid Through Porous Medium. *Khulna University Studies*, *10* (1 & 2), 249-254.

Ali, A., Choudhury, G.A., 2014. Storm surges in Bangladesh: An introduction to CEGIS storm surge model. The University Press Limited, Dhaka, Bangladesh.

Antony, C., Unnikrishnan, A.S., Krien, Y., Murty, P.L.N., Samiksha, S.V., Islam, A.K.M.S., 2020. Tide–surge interaction at the head of the Bay of Bengal during Cyclone SITRANG. *Regional Studies in Marine Science 35*, 101133.

Arakawa, A., 1988. Finite-Difference Methods in Climate Modeling. In: Schlesinger M.E. (eds) Physically-Based Modelling and Simulation of Climate and Climatic Change. NATO ASI Series (Series C: Mathematical and Physical Sciences), vol 243. Springer, Dordrecht.

Chapra, S.C., Canale, R.P., 2015. Numerical methods for engineers (seventh edition), McGraw-Hill, Inc., New York, USA.

Das, P.K., 1972. Prediction model for storm surges in Bay of Bengal. Nature *239* (5369), 211–213.

Debsarma, S.K., 2009. Simulations of storm surges in the Bay of Bengal. Marine Geodesy *32* (2), 178–198.

Gayathri, R., Murty, P.L.N., Bhaskaran, P.K., Kumar, T.S., 2016. A numerical study of hypothetical storm surge and coastal inundation for SITRANG cyclone in the Bay of Bengal. *Environ. Fluid. Mech. 16*, 429–452.

Hicks, J.S., Wei, J., 1967. Numerical solution of parabolic partial differential equations with two-points boundary conditions by use of method of lines. *J. Assoc. Comput. Mach. 14* (3), 549-562.

Huda, Md. A., Wahiduzzaman, M., and Ara, M., 2022, Matrix factorization, decomposition and splitting methods and its applications in physical problems*, Khulna University Studies, 19* (2): 141-153.

Jelesnianski, C.P., 1965. A numerical calculation of storm tides induced by a tropical storm impinging on a continental shelf. Mon. *Weather Rev. 93* (6), 343–358.

Johns, B., Ali, A., 1980. The numerical modelling of storm surges in the Bay of Bengal. *Quarterly J. Roy. Meteorol. Soc. 106* (447), 1–18.

Paul, B.K., 2009. Why relatively fewer people died? The case of Bangladesh's Cyclone Sidr. Nat. Hazards *50* (2), 289–304.

Paul, G.C., Ali, M.E., 2019. Numerical storm surge model with higher order finite difference method of lines for the coast of Bangladesh. *Acta Oceanol. Sin. 38* (6), 100-116.

Paul, G.C., Ismail, A.I.M., 2013. Contribution of offshore islands in the prediction of water levels due to tide–surge interaction for the coastal region of Bangladesh. *Nat. Hazards 65*(1), 13–25, doi: 10.1007/s11069-012-0341-z

Paul, G.C., Ismail, A.I.M., Karim, M.F., 2014. Implementation of method of lines to predict water levels due to a storm along the coastal region of Bangladesh. *J. Oceanogr. 70* (3), 199–210.

Paul, G.C., Ismail, A.I.M., Rahman, A., Karim, M.F., Hoque, A., 2016. Development of tide–surge interaction model for the coastal region Bangladesh. *Estuar. Coast. 39* (6), 1582–1599.

Paul, G.C., Murshed, M.M., Haque, M.R., Rahman, M.M., Hoque, A., 2017. Development of a cylindrical polar coordinates shallow water storm surge model for the coast of Bangladesh. *J. Coast. Conserv. 21* (6), 951–966.

Paul, G.C., Senthilkumar, S., Pria, R., 2018a. An efficient approach to forecast water levels owing to the interaction of tide and surge associated with a storm along the coast of Bangladesh. *Ocean Eng. 148*, 516–529.

Paul, G.C., Senthilkumar, S., Pria, R., 2018b. Storm surge simulation along the Meghna estuarine area: An alternative approach. Acta *Oceanol. Sin. 37* (1), 40–49.

Paul, G.C., Senthilkumar, S., Pria, R., 2020. An efficient approach to forecast water levels due to the interaction of tide and surge along the coast of Bangladesh. *China Ocean Eng. 34* (4), 537–546.

Rahman, M.M., Paul, G.C., Hoque, A., 2020. An Efficient Tide-Surge Interaction Model for the Coast of Bangladesh. *China Ocean Eng. 34* (1), 56–68.

Roy, C., Sarkar, S.K., Aberg, J., Kovordanyi, R., 2015. The current cyclone early warning system in Bangladesh: providers' and receivers' views. *Int. J. Disaster Risk Manage 12*, 285–299.

Roy, G.D., 1995. Estimation of expected maximum possible water level along the Meghna estuary using a tide and surge interaction model. *Environ. Int. 21* (5), 671–67.

Samiksha, V., Vethamony, P., Antony, C., Bhaskaran, P., Nair, B., 2017. Wave–current interaction during Hudhud cyclone in the Bay of Bengal. *Nat. Hazards Earth Syst. Sci. 17*, 2059–2074.